Diminished Medium-Range Order Observed in Annealed Amorphous Germanium

J. M. Gibson
Departments of Physics and Materials Science, University of Illinois, 104 S. Goodwin Avenue, Urbana, Illinois 61801

M. M. J. Treacy
NEC Research Institute, Inc., 4 Independence Way, Princeton, New Jersey 08540
(Received 4 November 1996)

We use variable coherence transmission electron microscopy to examine medium-range ordering in vacuum-deposited amorphous germanium. The method accesses higher-order atomic correlations through statistical analysis of hollow-cone dark-field image speckle. This yields greater sensitivity to medium-range order than the familiar pair correlation function obtained from diffraction. We find that thermal annealing of amorphous germanium reduces the degree of medium-range order, affirming the thermodynamic stability of the random network. [S0031-9007(97)02365-X]

PACS numbers: 61.14.Rq, 61.16.Bg, 61.43.–j

The absence of information on higher-order atomic correlations is a serious obstacle to the deeper understanding of amorphous structures [1]. Although diffraction studies elucidate short-range order in amorphous materials [2–4], their output, the atom pair-correlation function [5], is insensitive beyond short range. Exploiting the sensitivity of higher-order atomic correlations to medium-range order, we use a microscopy method to show that medium-range order on the 1–2 nm scale is diminished after annealing of deposited amorphous germanium. Increased short-range order comes at the expense of medium-range order, and implies that the annealed specimen better approximates a continuous random network (CRN). This result illustrates the stability of the CRN against medium-range ordering [6].

Our method, variable coherence microscopy, measures the statistical properties of transmission electron microscope (TEM) hollow-cone dark-field images. From the beginnings of atomic resolution TEM, it has been believed that direct images of disordered materials elucidate atomic structure without being subject to the macroscopic averaging of diffraction experiments. Early work showed that visual inspection of images was unreliable, as random effects could qualitatively simulate ordering [7,8]. Even though the macroscopic averaging of diffraction experiments is avoided in high-resolution TEM, there is a form of mesoscopic averaging through a volume characterized laterally by the microscope resolution, and vertically by the specimen thickness, often containing $\sim$1000 atoms. Although fluctuations in the scattering from such volumes are important they can be characterized only by statistical analysis [9]. Modern technology for image recording and processing enables such experiments. Variable coherence electron microscopy exploits the nonlinearity of dark-field imaging. Because of this nonlinearity, higher-order atomic correlations are detectable from simple statistical properties such as the variance of image intensity. Illumination coherence provides a valuable experimental variable. Alternative quantitative approaches to microscopy and microdiffraction of amorphous materials, which do not exploit variable coherence, have also been discussed [10,11]. Another method to obtain higher-order correlation functions from x-ray absorption spectroscopy has additionally been identified [12].

On the basis of pair correlation functions, it has been determined that the amorphous tetrahedral semiconductors Si and Ge can be classed as continuous random networks [3,13]. Calorimetric studies have shown that amorphous Ge undergoes a significant structural relaxation on thermal annealing below the crystallization temperature [14]. In fact, up to 50% of the heat of crystallization can be evolved. This dramatic relaxation was originally noted for ion-implanted Ge, but has since been detected in varying degrees for deposited amorphous semiconductor films [15]. Structural analysis of the effect of annealing shows a modest reduction in the degree of bond-angle disorder, that is, an increase in short-range order. It has been assumed that this coincides with a general increase in medium-range ordering, although there was no experimental data to support the idea. Our results, for evaporated Ge films, show that the opposite occurs: Medium-range order is diminished on thermal relaxation. We speculate that a CRN is difficult to nucleate during vapor deposition, but is the lowest energy state for amorphous tetrahedral semiconductors. Consequently, as-deposited films contain a granular structure with medium-range order which is reduced on annealing.

The variable coherence microscopy technique is described in detail elsewhere [16]. Dark-field images, characterized by intensity distributions $I(\boldsymbol{r}, \kappa)$, are recorded with partially coherent illumination in a TEM. Coherence is controlled by the hollow-cone illumination method [17]. Statistical properties of images are measured as a function of κ, the coherence parameter. κ is determined by the inner semiangle α of the hollow-cone illumination and is of approximate magnitude α/λ, with λ being the electron

 0031-9007/97/78(6)/1074(4)$10.00

wavelength. The kinematical diffraction approximation, which is valid for thin (<30 nm) amorphous specimens [18], predicts the normalized variance of an image from an area containing N atoms to be [16]

$$V = \frac{\langle I^2(\boldsymbol{r},\boldsymbol{\kappa})\rangle}{\langle I(\boldsymbol{r},\boldsymbol{\kappa})\rangle^2} - 1 = N_0 \frac{\sum_{j,l,m,n=1}^{N} A_{jn}A_{nl}A_{mn}F_{jl}F_{mn}}{\left[\sum_{p,q=1}^{N} A_{pq}F_{pq}\right]^2} - 1, \qquad (1)$$

where N_0 is the number of pixels in the image. F_{jl} is the coherence strength and A_{jl} is the microscope response function, which is of the order of the image pixel size. Both F_{jl} and A_{jl} are localized functions of the atom-pair separation $\boldsymbol{r}_{jl}$ so that the upper and lower sums in Eq. (1) probe mesoscopic volumes. V depends on the joint probability distribution function of up to four atoms j, l, m, and n. It is possible to approximate Eq. (1) in a form that involves no higher than three-body correlations. The mean intensity $\langle I(\boldsymbol{r},\boldsymbol{\kappa})\rangle$, which is equivalent to the diffracted intensity averaged over the image acceptance angles, is dependent only on the pair distribution function. Intuitively, the image is sensitive to spatial fluctuations, whereas the diffraction pattern is limited to the averaged pair correlation function. Medium-range order is best emphasized when the microscope resolution approximates the correlation length, and not at the highest possible resolution.

Consider one form of the three-body correlation function, that is $\rho(\boldsymbol{r}_2 \mid \boldsymbol{r}_1)$, which expresses the conditional probability of there being an atom at $\boldsymbol{r}_2$ given an atom at $\boldsymbol{r}_2$ from an atom at the origin. It is not widely recognized that this function has far greater sensitivity to medium-range order than the pair correlation function. To illustrate the point, we simulated a uniformly distributed static disorder of maximum value 0.1 nm added to each atom in a germanium crystal. Figure 1 shows that, whereas the pair correlation function is almost structureless beyond 1 nm, the three-body correlation function reveals the long-range periodicity. The absence of medium- or long-range structure in the pair correlation function comes from the overlap of an increasing number of possible interatom correlations at large distances. The three-body correlation was calculated here for $\boldsymbol{r}_1$ being the edge vector of the local germanium tetrahedron. In a sense, the three-body correlation function is "smart" in that it adapts to the local environment. We have done similar calculations with amorphous models which reveal the same sensitivity. If one rotates into the local frame of reference of the highly ordered nearest neighbor in an amorphous semiconductor, the structure reveals greater medium-range order. Consequently, we would expect from Eq. (1) that the image speckle statistics would be particularly sensitive to the extent of medium-range order.

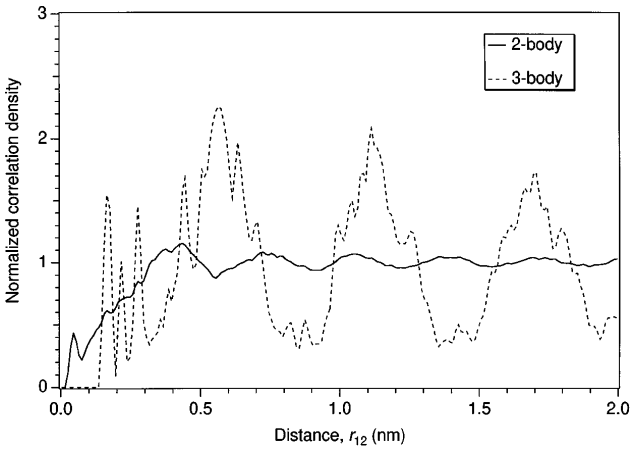

FIG. 1. Simulations of the two-body and three-body correlation functions of a Ge crystal that has randomized 0.1 nm disorder at each atom site. Note that the three-body correlation more clearly reveals the underlying order.

Amorphous Ge was evaporated at a rate of 0.8 nm/min from a BN crucible onto freshly cleaved rock salt at room temperature. The vacuum during deposition was 2×10^{-10} torr. These 20 nm thick films were floated onto Cu support grids and examined in a Hitachi H9000NAR TEM operating at 200 kV. Images were recorded on a Gatan 689/690 slow-scan CCD camera, at a magnification equivalent to 0.63 nm per CCD pixel, and with ~500 counts per CCD pixel. Intensity variance V was obtained by integrating the image power spectral density over a frequency (1/length) range 0.1–0.5 nm^{-1}. The lower frequency limit eliminates the deleterious effects of both the illumination nonuniformity and any macroscopic specimen structure. The upper limit, combined with a relatively fixed average count per image, renders negligible the effect of electron shot noise. The CCD modulation transfer function was deconvolved from the data [19], which therefore represent true electron intensity statistics. The width of the microscope response function A_{jl}, or image resolution, was set at either 1.7 or 0.6 nm by choice of an objective aperture. The coherence strength F_{jl} is continuously scalable through electronic control of the inner angle of hollow-cone illumination. Over a prolonged period, coarse-scale etching occurred under irradiation, but had negligible effect in the frequency range of interest. Previous experiments showed that specimen thickness has little effect on normalized variance [16]. After initial TEM observation, samples were vacuum-annealed *in situ* at 350 °C for 15 min.

Figure 2 shows the normalized speckle variance from a 20 nm thick *a*-Ge film, before and after thermal annealing. In both cases, peaks appear at κ values of ~3.1 and ~5.8 nm^{-1} coincident with peaks in the diffraction pattern. These data were taken with a microscope response function A_{jl} of width 1.7 nm. Experiments on the same samples using an A_{jl} width of 0.6 nm show less speckle

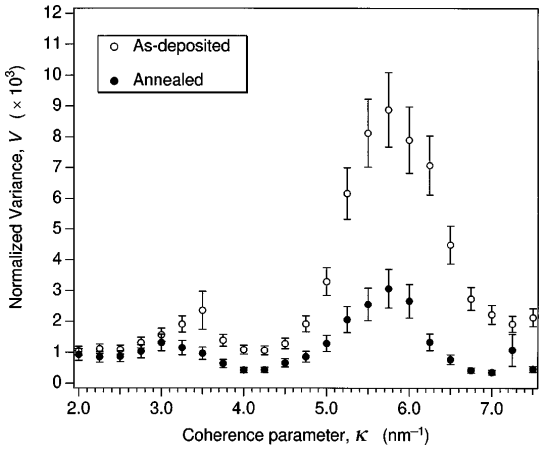

FIG. 2. Plots of the normalized variance of hollow-cone dark-field TEM images from a 20 nm thick *a*-Ge film before and after annealing. Medium-range order, exemplified by the peak at $\kappa \approx 5.8$ nm^{-1}, is diminished after annealing.

and no peaks at these positions. It is helpful to think of the $F_{jl}(\kappa)$ coherence strength terms as probing the ordering on a scale $1/\kappa$, while simultaneously the A_{jl} terms probe the medium-range correlations. A peak in V for a given A_{jl} implies ordering at the length scale of A_{jl}. Computations on model systems using Eq. (1) also show that there must be atomic correlations within the Ge extending beyond 1 nm in order to produce these peaks. Simulations using the Wooten-Winer-Weaire CRN model [20], for example, do not show such medium-range structure [16]. In addition, prior work on the anisotropy of CRN models showed that they were statistically indistinguishable from a completely random distribution of atoms [21]. Annealing the sample reduces the variance peak intensities significantly, thus we conclude that medium-range order is diminished in *a*-Ge on annealing. Note that temperature-related changes in the diffraction pattern are much more subtle but have been interpreted as modest improvements in short-range order [3]. Experiments on *a*-Ge and *a*-Si deposited on polymethyl methacrylate under differing vacuum conditions gave qualitatively similar results. Preliminary results on ion-implanted *a*-Si also show the effect.

Figure 3 shows two of the dark-field images from which Fig. 2 was obtained. Both are from an unannealed sample, with Fig. 3(a) taken at the $\kappa \approx 5.8$ nm^{-1} peak, and Fig. 3(b) at the $\kappa \approx 4.0$ nm^{-1} dip. The difference in intensity variance is clear. Three additional features are noteworthy: (1) a fine-scale structure (speckle) at $\sim$2 nm; (2) a dendritic structure at $\sim$20 nm, which has been observed previously and is associated with voids [22]; (3) linear features, which correspond to steps on the cleaved rock-salt surface. Only (1) contributes to the measured variance, and is suppressed in Fig. 3(b). We also observed a low density of germanium crystallites of $\sim$10 nm size whose number increased slightly on

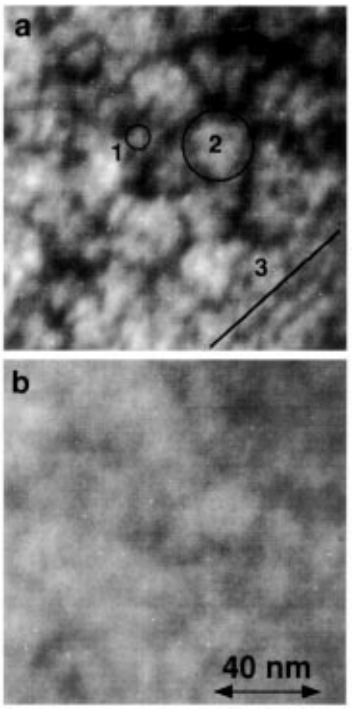

FIG. 3. Hollow-cone dark-field images from the same area of a 20 nm thick unannealed *a*-Ge film. (a) Maximum variance, $\kappa \approx 5.8$ nm^{-1}. (b) Minimum variance, $\kappa \approx 4.0$ nm^{-1}.

annealing. These are avoided in the measurements. Tsu [23], using a variety of indirect observations, has also suggested the effect reported here.

Figure 2 shows a drop by a factor of 3 in the speckle variance peak at 5.8 nm^{-1} after annealing. Since a structure without medium-range ordering would exhibit no peaks in the speckle variance we conclude that a major reduction in the degree of medium-range order has occurred. Experiments by others on similar amorphous semiconductor films [15] show considerable heat evolution on annealing. Lannin [24,25], using Raman spectroscopy, has shown increased short-range order after annealing. Temkin *et al.* [3] found the same effect for *a*-Ge deposited at higher temperatures. It has been concluded from such studies [25] that reduction in bond angle disorder is a significant contributor to the free energy reduction on annealing. It has widely been supposed that increased short-range order implied increased medium-range order. Our experiments are the first to directly address this issue, but reach the opposite conclusion.

Can we explain this conundrum? A question that has puzzled several theorists in the past is—how does a random network nucleate [26,27]? Even though the random network may be metastable, it is difficult to imagine a handful of atoms nucleating with such disorder. Gaskell [26] proposed a noncrystalline, but highly ordered granular structure, which was later found to be inconsistent with the measured pair-correlation function. Phillips [27] similarly proposed clusterlike structures for other amorphous

semiconductors. We suggest that a granular structure of ~2 nm scale is formed during low temperature deposition of *a*-Ge and *a*-Si. A large density of nucleation centers with a quasiordered structure forms. As these grow and impinge on each other, excessive interfacial energy results from their random relative orientations. At this point we postulate that a true random network with uniformly distributed strain energy has a lower free energy. This is supported by simulations showing grain boundary amorphization in Si [28]. However, this transition would require thermal activation. Although we do not propose that the as-deposited state is nanocrystalline, our data reveal medium-range order which is not consistent with a random network model. On annealing, this granularity is greatly attenuated, and the structure better resembles a random network. The CRN is indeed the lowest energy state of amorphous tetrahedral semiconductors. Our observation that as-deposited amorphous films have more medium-range order than the CRN, has likely implications to understanding the properties of *a*-Si(H) photovoltaics. Instabilities in the electrical properties under UV radiation [29] may be related to medium-range order and thermal annealing.

Our technique permits systematic study of a variety of materials and annealing conditions. It is desirable to have computer models representing the as-deposited phase. In the future we hope to obtain directly details of the higher-order correlation functions from our approach. One can also envisage closely related "fluctuation microscopy" techniques. In variable resolution microscopy, for example, the A_{jl} functions are continuously varied at fixed coherence F_{jl}. This would allow direct extraction of the medium-range order correlation length, but is challenging experimentally.

In summary, variable coherence TEM revealed medium-range ordering in vacuum-deposited *a*-Ge. After annealing, the medium-range order was diminished. Our method achieves its sensitivity to medium-range order by accessing atomic correlations of higher order than the widely used pair correlation function. Our observation that thermal annealing of amorphous germanium reduces the degree of medium-range order, establishes the thermodynamic stability of the random network.

The authors wish to thank Dave Loretto, Fred Wooten, Peter Miller, Dale Jacobson, and Peggy Bisher.

[1] N. E. Cusack, *The Physics of Structurally Disordered Matter* (Adam Hilger, Bristol, United Kingdom, 1987), p. 23.
[2] S. C. Moss and J. F. Graczyk, Phys. Rev. Lett. **23**, 1167 (1969).
[3] R. J. Temkin, W. Paul, and G. A. N. Connell, Adv. Phys. **22**, 581 (1973).
[4] G. Etherington, A. C. Wright, J. T. Wenzel, J. C. Dore, J. H. Clarke, and R. N. Sinclair, J. Non-Cryst. Solids **48**, 265 (1982).
[5] B. E. Warren, *X-Ray Diffraction* (Addison-Wesley, Reading, Massachusetts, 1959).
[6] W. H. Zachariasen, J. Am. Chem. Soc. **54**, 3841 (1932).
[7] M. L. Rudee and A. Howie, Philos. Mag. **25**, 1001 (1972).
[8] P. Chaudhari and J. F. Graczyk, in *Proceedings of the 5th International Conference on Amorphous and Liquid Semiconductors* (Taylor and Francis, London, 1973), Vol. 1, p. 59.
[9] W. Cochran, Phys. Rev. B **8**, 623 (1973).
[10] G. Y. Fan and J. M. Cowley, Ultramicrosopy **17**, 345 (1985); **24**, 49–60 (1988).
[11] J. M. Rodenburg, Inst. Phys. Conf. Ser. **78**, 103 (1985).
[12] A. Filipponi, F. Evangelisti, M. Benefatto, S. Mobilio, and C. R. Natoli, Phys. Rev. B **40**, 9636 (1989).
[13] D. E. Polk, J. Non-Cryst. Solids **5**, 365–376 (1971).
[14] E. P. Donovan, F. Spaepen, D. Turnbull, J. M. Poate, and D. C. Jacobson, J. Appl. Phys. **57**, 1795 (1985).
[15] R. R. De Avillez, L. A. Clevenger, and C. V. Thompson, J. Mater. Res. **4**, 1057 (1989).
[16] M. M. J. Treacy and J. M. Gibson, Acta Crystallogr. Sect. A **52**, 212 (1996).
[17] W. Krakow and L. A. Howland, Ultramicroscopy **2**, 53–67 (1976).
[18] L. D. Marks, Ultramicroscopy **30**, 25 (1988).
[19] O. L. Krivanek, P. H. Gaskell, and A. Howie, Nature (London) **262**, 454 (1976).
[20] F. Wooten, K. Winer, and D. Weaire, Solid State Phys. **40**, 1 (1987).
[21] R. Alben, G. S. Cargill, and J. Wenzel, Phys. Rev. B **13**, 835 (1976).
[22] P. Viscor, J. Non-Cryst. Solids **101**, 156 (1988); **101**, 170 (1988).
[23] R. Tsu, J. Non-Cryst. Solids **97&98**, 163 (1987).
[24] J. S. Lannin, in *Semiconductors and Semimetals*, edited by J. I. Pankove (Academic, New York, 1984), Vol. 21B, p. 175.
[25] J. Fortner and J. S. Lannin, Phys. Rev. B **37**, 10 154 (1988).
[26] P. H. Gaskell, J. M. Gibson, and A. Howie, in *The Structure of Non-Crystalline Materials* (Taylor and Francis, London, 1977), p. 181.
[27] J. C. Phillips, J. Non-Cryst. Solids **34**, 153 (1979).
[28] D. Wolf, J. Wang, S. R. Phillpot, and H. Gleiter, Phys. Rev. Lett. **74**, 4686 (1995).
[29] D. L. Staebler and C. R. Wronski, Phys. Rev. Lett. **31**, 22 (1977).